AD-A091 518 NAVAL OCEAN SYSTEMS CENTER SAN DIEGO CA F/G 4/2
SURFACE BASED REMOTE SENSING IN MARINE AIR. EXTENSIVE ANALYSIS --ETC(U)
AUG 80 V R NOONKESTER
UNCLASSIFIED NOSC/TR-580 NL

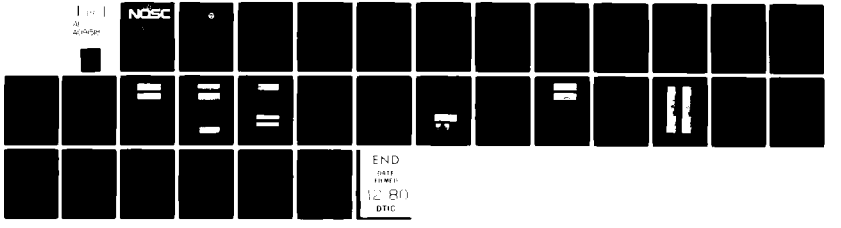

LEVEL II

12

NOSC

NOSC TR 580

AD A091518

NOSC TR 580

Technical Report 580

SURFACE BASED REMOTE SENSING IN MARINE AIR

Extensive analysis of echoes by several sensors reveals evolutionary atmospheric processes related to weather capable of affecting naval operations

VR Noonkester

1 August 1980

Research Report: July 1971-January 1980

Prepared for:
Naval Air Systems Command

DDC FILE COPY

Approved for public release; distribution unlimited.

NAVAL OCEAN SYSTEMS CENTER
SAN DIEGO, CALIFORNIA 92152

80 10 31 025

NAVAL OCEAN SYSTEMS CENTER, SAN DIEGO, CA 92152

AN ACTIVITY OF THE NAVAL MATERIAL COMMAND

SL GUILLE, CAPT, USN
Commander

HL BLOOD
Technical Director

ADMINISTRATIVE INFORMATION

Work was performed under NOSC 61153N, WRO330200, 532-MP04, from July 1971 to January 1980, and was sponsored by Naval Air Systems Command.

Released by
JH Richter, Head
Electromagnetic Propagation Division

Under authority of
JD Hightower, Head
Environmental Sciences Department

ACKNOWLEDGEMENTS

The author is indebted to many people who have developed, tested, improved, operated and maintained the sensors, have collected data with considerable efficiency and competence, have obtained high quality supporting meteorological data, have processed and analyzed the data and have documented interpretations. The major contributors to these accomplishments include: EE Gossard (now at NOAA), WK Horner, HG Hughes, DR Jensen and ML Phares. Particular recognition is extended to JH Richter for his intimate involvement in all aspects of the investigations.

UNCLASSIFIED

SECURITY CLASSIFICATION OF THIS PAGE *(When Data Entered)*

REPORT DOCUMENTATION PAGE

READ INSTRUCTIONS BEFORE COMPLETING FORM

1. REPORT NUMBER: NOSC Technical Report 580 (TR 580)	2. GOVT ACCESSION NO.: AD-A097 528
3. RECIPIENT'S CATALOG NUMBER:	
4. TITLE *(and Subtitle)*: SURFACE BASED REMOTE SENSING IN MARINE AIR. Extensive analysis of echoes by several sensors reveals evolutionary atmospheric processes related to weather capable of affecting naval operations.	5. TYPE OF REPORT & PERIOD COVERED: Research Report. July 1971 - January 1980
	6. PERFORMING ORG. REPORT NUMBER:
7. AUTHOR(s): VR Noonkester	8. CONTRACT OR GRANT NUMBER(s): WR 03302
9. PERFORMING ORGANIZATION NAME AND ADDRESS: Naval Ocean Systems Center, San Diego, CA 92152	10. PROGRAM ELEMENT, PROJECT, TASK AREA & WORK UNIT NUMBERS: 61153N, WR033020, S32-MP04
11. CONTROLLING OFFICE NAME AND ADDRESS: Naval Air Systems Command, Washington, DC 20361	12. REPORT DATE: 1 August 1980
	13. NUMBER OF PAGES: 30
14. MONITORING AGENCY NAME & ADDRESS *(if different from Controlling Office)*: NOSC/TR-580	15. SECURITY CLASS. *(of this report)*: UNCLASSIFIED
	15a. DECLASSIFICATION/DOWNGRADING SCHEDULE:

16. DISTRIBUTION STATEMENT *(of this Report)*
Approved for public release; distribution unlimited.

17. DISTRIBUTION STATEMENT *(of the abstract entered in Block 20, if different from Report)*

18. SUPPLEMENTARY NOTES

19. KEY WORDS *(Continue on reverse side if necessary and identify by block number)*
Remote sensing
Boundary layer meteorology
Meteorological phenomena

20. ABSTRACT *(Continue on reverse side if necessary and identify by block number)*
Extensive analysis of echoes by several sensors reveals evolutionary atmospheric processes related to weather capable of affecting naval operations.

DD FORM 1 JAN 73 1473 EDITION OF 1 NOV 65 IS OBSOLETE
S/N 0102-LF-014-6601

UNCLASSIFIED
SECURITY CLASSIFICATION OF THIS PAGE *(When Data Entered)*

OBJECTIVE

Investigate the nature of small-scale, low-level, atmospheric processes revealed by various remote sensors and the relation of these processes to meso- and synoptic scale processes, and determine the extent the information can improve the performance of Fleet systems. In particular, investigate the capability of surface-based remote sensors to monitor the evolutionary processes related to clouds, fog, turbulence, aerosols and radar ducting in marine air. Also, evaluate the operational potential of remote sensors for the Navy.

RESULTS

The major results of investigations ~~extending from 1971 to 1980~~ include: (1)

- Evaluation of the following surface-based remote sensors, either singularly, jointly, or separated in several coastal regions:
  - Fixed, vertical pointing FM-CW radar,
  - Mobile, scanning FM-CW radar,
  - Acoustic monostatic echosounder,
  - Acoustic, bistatic wind sensing system,
  - Lidar,
  - High powered pulsed radar, and
  - Ceilometer using nonstandard film recording technique; (2)
- Determination of advantages and complementary features of sensors; (3)
- Identification of echoes and their evolution related to significant meteorological processes potentially affecting naval operations:
  - Temperature and relative humidity inversion base height,
  - Stratus cloud top,
  - Echo structure, including drizzle, beneath stratus clouds leading to fog formation,
  - Turbulence related to waves, forced and free convection, and aircraft wing-tip vortices, and
  - Extrapolation of ascending convective mixing layer depth to condensation level where clouds form and descending subsidence inversion base or wind shear region into and through stratus clouds or fog deck to instigate cloud/fog dissipation, and (4)
- Development of echo coding technique for transmitting essential echo features and acquiring an echo climatology.

RECOMMENDATIONS

- Continue to develop remote sensors, and use them to investigate atmospheric processes at coasts and islands – particularly those capable of aerosol assessments.
- Continue to investigate the relations between processes at different atmospheric scale sizes (microscale, mesoscale, and synoptic scale) and sensor echo evolution.

CONTENTS

INTRODUCTION

A new era in the remote probing of atmospheric boundary layer processes began when McAllister (1968) (ref 1) reported on an acoustic echosounder technique and Richter (1969) (ref 2) reported on a radar (Frequency-Modulated, Continuous-Wave (FM-CW)) technique for observing atmospheric structural details in clear air at close range ($\sim$ 80 m) with a high range resolution (FM-CW radar: $\sim$ 1 m max.; acoustic echosounder: $\sim$ 3 m max.). These techniques have provided information on significant boundary-layer processes in unprecedented detail on a continuous basis at altitudes normally below 1 km. The more economical acoustical echosounder principally monitors backscatter from regions of turbulent mixing of potential temperature θ ($\Delta\theta/\Delta z \neq 0$) while the FM-CW radar monitors backscatter from regions of turbulent mixing of moisture e ($\Delta e/\Delta z \neq 0$). Both techniques can accurately measure the wind component carrying the turbulent region in the direction of the probing beam using doppler techniques (acoustic: Beran, et al., 1974 (ref 3); FM-CW radar: Chadwick, et al., 1976 (ref 4)). Acoustic bistatic systems (Jensen and Richter, 1976 (ref 5); Beran, et al., 1974 (ref 3)) have also been used to measure the horizontal wind vector.

Thousands of hours of FM-CW radar data and hundreds of hours of acoustic data have been taken by the Naval Ocean Systems Center (NOSC) at various coastal regions, principally in Southern California, concurrently with standard surface meteorological data, including radiosondes, and intermittently with other remote sensors (eg, FM-CW radar and lidar: Noonkester, et al., 1974 (ref 6); FM-CW radar, acoustic echosounder, airborne sensors and high-powered pulsed radar: Richter, et al., 1974 (ref 7)). These data have been examined relative to turbulence, convection, refractive index structure, stratus clouds, cloud thickness, fog, wind shear, sea breeze, aircraft wing-tip vortices, mesoscale and synoptic changes, and similarities and differences in sensors. Results have been documented in many reports. A technique for coding these echoes has been proposed (Noonkester, 1979a) (ref 8) and can be used to convey essential echo information and to compile climatological data.

The purpose of this report is to present a review of significant meteorological information available from surface-based remote sensors used by NOSC in coastal regions and to suggest a few possible operational uses of the sensors.

---

[1]McAllister, L.G., 1968: Acoustic sounding of the lower troposphere. J. Atmos. and Terr. Phys., 30, 1439-1440.

[2]Richter, J.H., 1969: High resolution tropospheric radar sounding. Radio Sci., 4, 1261-1268.

[3]Beran, D.W., B.C. Willmarth, F.C. Carsey and F.F. Hall, Jr., 1974: An acoustic doppler wind measuring system. J. Acoustic. Soc. Am., 55, 334-338.

[4]Chadwick, R.B., K.P. Moran, R.G. Strauch, G.E. Morrison and W.C. Campbell, 1976: A new radar for measuring winds. Bull. Am. Meteor. Soc., 57, 1120-1125.

[5]Jensen, D.R. and J.H. Richter, 1976: Evaluation of a Xonics Acoustic Echosounder and Wind Sensing System. Naval Electronics Laboratory Center Tech. Report 1997.

[6]Noonkester, V.R., D.R. Jensen, J.H. Richter, W. Viezee and R.T.H. Collis, 1974: Concurrent FM-CW radar and lidar observations of the boundary layer. J. Appl. Meteor., 13, 249-256.

[7]Richter, J.H., D.R. Jensen, V.R. Noonkester, T.G. Konrad, A. Arnold and J.R. Rowland, 1974: Clear air convection: A close look at its evolution and structure. Geophys. Res. Lett., 4, 173-176.

[8]Noonkester, V.R., 1979a: A technique for coding boundary layer echoes from surface-based remote sensors. Bull. Am. Meteor. Soc., 60, 20-27.

SENSORS AND DATA

The major surface-based remote sensors employed in coastal studies by NOSC have been FM-CW radars, both a fixed and scanning/mobile radar, an acoustic echosounder, and an acoustic bistatic wind sensing system. The FM-CW radar receives backscatter from regions of turbulent mixing along a nonzero gradient of the radio refractive index which is essentially a function of the humidity. Operating near 3 GHz, the radar receives backscatter from regions of turbulent mixing near a scale size of 5 cm in the inertial subrange of a turbulent cascade. The range resolution was usually set to 2 m and the range gate was usually set to extend from 80 m to about 700 m. The data were recorded by filming an intensity modulated scope displaying the backscatter using a shutterless movie camera. Although the filmed data are qualitative, the large dynamic range of the filmed record provides a large relative range of echo intensity. Richter, 1969 (ref 2) and Richter, et al., 1972 (ref 9) give details about the characteristics and performance of the fixed and the scanning/mobile radars respectively.

The acoustic backscatter sounder receives acoustic energy from regions of turbulent mixing along a nonzero gradient of the acoustic refractive index. Although the contribution of the correlated fluctuations in temperature and humidity to the backscattered energy may not always be insignificant (Wesely, 1976) (ref 10), the major source of backscatter is assumed to be caused by potential temperature fluctuations. The turbulent scale size producing backscatter for the 2 kHz NOSC sounder is about 7 cm. The range resolution was usually set to 34 m in a height window almost identical to the radar height window. The echoes were recorded on film in the same manner as for the radar echoes.

Two, fan-beam, bistatic acoustic receivers were placed at about 400 m north and west of the vertically pointing acoustic transmitter. The fan beams were oriented to mutually receive sidescattered acoustic energy between elevations of about 100 to 500 m above the transmitter. The energy scattered to the bistatic receivers is doppler shifted because the horizontal and vertical wind transports the vertically transmitted pulse. The east-west and north-south horizontal wind components are computed for seven elevations, which are separated by about 60 m, by using the doppler shift at each receiver (backscatter and bistatic) for each elevation. Vertical winds are determined by the doppler shift of the backscattered signal received at the transmitter. The winds are obtained by averaging over about 10 to 20 pulses when pulsing every 6 sec. Acoustic wind profiles are normally computed every 30 min, but are computed more frequently for selected periods. Jensen and Richter, 1976 (ref 5) discuss details of the acoustic sounder and wind sensing system. Table 1 summarizes aspects of these sensors.

Other measurements available at NOSC include temperature, dew point, wind, visibility (MRI 1580A; and transmissometer, AN/GMQ 13C), ceiling (ceilometer, AN/GMQ 13C) and upper atmosphere structure (radiosondes, with or without winds). Radiosondes are released at 0400 and 1600 PST from the National Oceanographic and Atmospheric Administration (NOAA) station at Montgomery Field (MYF) (18 km NE of NOSC). The ceilometer data, recorded by the filming technique used for the radar and acoustic backscatter signals, provide details on cloud heights at low elevations. A facsimile recorder provides NOAA synoptic information and the nearby Naval Weather Service Facility, at North

---

[9] Richter, J.H., D.R. Jensen and M.L. Phares, 1972: Scanning FM-CW radar sounder. The Review of Scientific Instruments, 43, 1623-1625.

[10] Wesely, M.L., 1976: The combined effect of temperature and humidity fluctuations on refractive index. J. Appl. Meteor., 15, 43-49.

Sensor	Operational Frequency	Range Resolution	Pulse Repetition Rate	Primary Scattering Element	Primary Height Range	Primary Recording Technique
FM-CW Radar; Fixed and mobile	3 GHz	1 m max.	100 ms (Signals ave. over secs.)	Turbulent moisture mixing	~ 80-700 m	Film
Acoustic Echo-sounder	2 kHz	1.7, 8.6, and 34 m	4, 6 s	Turbulent temperature mixing	~ 80-700 m	Film
Acoustic Wind Sensor System; Total wind vector	2 kHz	--	4, 6 s	Temperature and velocity turbulence	100-500 m 7 levels; $\Delta z \cong 50, 60$ m	Printout on teletypewriter
Lidar* (SRI) Mark VIII (ruby)	0.694 μm wavelength	20 m	3, 6 s	Aerosols; particulates	~ 50m-1 km	Film

*Light detection and ranging

Table 1. Basic information on surface-based remote sensors used during NOSC studies in coastal regions.

Island in San Diego, provides local data, forecasting, and Defense Meteorological Satellite Program (DMSP) data. Airborne, simultaneous measurements of aerosol spectra (PMS ASSP-100), temperature, dew point and elevation have been made in the nearby marine boundary layer but have not yet been related to the remote sensor measurements.

Table 2 contains a summary of the major studies completed at NOSC using surface based remote sensors in coastal regions, gives the principal sensor(s) involved, the location(s) of the measurements, and a brief comment on the type of information obtained for each study group.

ECHO TYPES AND MIXING PROCESSES

FM-CW radar and acoustic echoes are analogous to cloud patterns in their many varieties and form and, just like clouds, distinct types are usually present. Several distinct types are often present simultaneously and rarely will the echo pattern have no recognizable feature. Distinct echo types have been associated with certain atmospheric structures and processes in research programs conducted at NOSC since 1968 and are listed in table 3 according to the sensors having observed the type. The code representing each echo type in table 3 follows a general coding technique proposed by Noonkester, 1979a (ref 8), who presented examples of each type and briefly discussed their meteorological meaning.

Studies involving in situ measurements and theory have shown that many significant boundary layer processes concern the turbulent mixing of air having different temperature and moisture characteristics. In general, FM-CW radar and acoustic echoes have been found to be from regions near or at boundaries of small or large scale air masses having a different potential temperature θ (acoustic), or moisture content e (radar) where wind shear is producing turbulence across the nonzero gradient of θ or e. The relationship between the magnitude of the combined gradient and wind shear required to produce a backscatter signal of a certain intensity has not been established. Rawinsondes do not reveal all gradients of θ or e and the associated wind shear where echoes are observed. Some data (Gossard, et al., 1971) (ref 11) have indicated that the scale size of some echo regions is smaller than the maximum 1 m resolution of the FM-CW radar.

Temperature inversions and convection are two prominent and significant boundary layer features and are usually observed by the radar and acoustic sounders. Some examples of echo structures revealing significant meteorological information related to inversions and convection are presented below.

METEOROLOGICAL INTERPRETATIONS

a. California stratus and inversion

Figure 1 shows an example of continuous acoustic and FM-CW radar echoes from the base of a subsidence inversion. Stratus clouds were present until 1625 GMT when the continuous echoes (S echoes) of both sounders intensified and broadened. An increase in

---

[11] Gossard, E.E., D.R. Jensen and J.H. Richter, 1971: An analytical study of tropospheric structure as seen by high-resolution radar. J. Atmos. Sci., 28, 794-807.

Major Studies	Principal Remote Sensors Involved	Location	Comments
1. Gravity and breaking Kelvin-Helmholtz waves	FM-CW radar	San Diego	Dynamics examined
2. Atmospheric processes creating echo types	FM-CW radar	San Diego, Salton Sea, Vandenberg AFB, San Francisco, and Wallops Island	Echo types identified
3. Atmospheric processes creating echo types and sensor comparison	a. FM-CW radar, acoustic echo-sounder	San Diego	Similar, complementary echoes
	b. FM-CW radar, acoustic echo-sounder, narrow-beam, high-power radar	Wallops Island	Convective activity and rise rates examined
	c. FM-CW radar, lidar	San Diego	Complementary information on waves, convection, turbulence, layers, etc.
4. Convective activity, also see 3b and 3c	FM-CW radar, acoustic echosounder	San Diego	Convective cell types identified; ocean-based convection observed
5. Aircraft wing-tip vortex	FM-CW radar	International Airport, San Diego	Vortex echo identified and motion modeled; statistics obtained
6. Marine fog	FM-CW radar, acoustic echosounder	San Diego	Fog formation processes identified

Table 2. Studies completed by NOSC using surface based remote sensors in coastal regions.

Major Studies	Principal Remote Sensors Involved	Location	Comments
7. Synoptic, mesoscale variations	FM-CW radar, fixed and mobile simultaneously	San Diego, Vandenberg AFB, San Nicolas Island	Surface marine layer depth variations
8. Wind measurements, total component	Acoustic bistatic wind system	San Diego	Turbulence, cloud dissipation, sea breeze

Table 2. Studies completed by NOSC using surface based remote sensors in coastal regions (continued).

Echo Type	Code**	Has been observed* during NOSC studies with: FM-CW Radar	Acoustic Echosounder	Lidar*** (SRI)	Atmospheric Information
Layer echoes					
Single-line echo	S	x	x	x	Near temperature inversion base Near stratus cloud top
Multiple-line echoes	M	x	x	x	Bottom layer near temperature inversion base Changing mesoscale conditions Gravity wave interactions
Layer action					
Waves	W	x	x	x	Gravity waves (periodic) Mesoscale changes (*nonperiodic*)
Breaking Kelvin-Helmholtz waves	W/	x	x	x	Richardson number < 0.25 in a stable, wind shear region Turbulence
Nonlayer features					
Free convection	C	x	x	x	Vertical mixing of heat, moisture, etc. Estimate time of cloud formation Turbulence, wind shear Haze layer
Forced convection	T	x			Near neutral stability Moderate to strong surface wind over rough topography Turbulence, no wind shear

*Different echoes may have been observed by other scientists, but they are not indicated

**Discussed by Noonkester, 1979a (ref 8)

***Usually observes echo type at boundary of aerosol layers and sometimes sees aerosol layers not bounded by echoes of other sensors

Table 3. Remote sensor echo types observed by NOSC in coastal regions.

Echo Type	Code	Has been observed during NOSC studies with			Atmospheric Information
		FM-CW Radar	Acoustic Echosounder	Lidar (SRI)	
Nonlayer features (cont)					
Thermal plumes	U	x	x	x	Strong surface heating and instability
Rain, drizzle	R	x	Antenna noise		Elevation of source Elevation of evaporation Elevation of wind shear
Other (nonlayer)					
Aircraft wing-tip vortex	F	x			Turbulence in vortex Contains aircraft pollution
Insects	I	x			Insects often congregate in layers sometimes associated with wind shear or near constant $\Delta T/\Delta Z$ Trajectory gives air motion

Table 3. Remote sensor echo types observed by NOSC in coastal regions (continued).

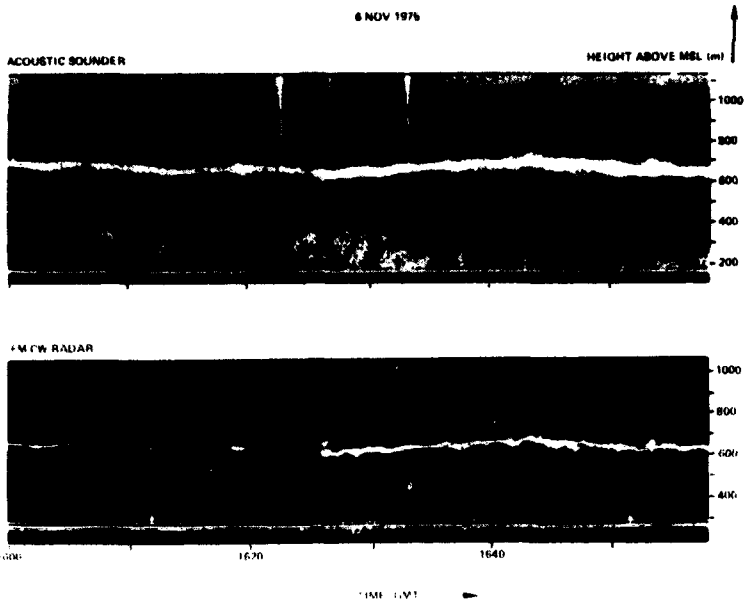

Figure 1. Simultaneous observations on the coast of San Diego. Stratus clouds with tops at 600 m dissipated at 1625 GMT.

the intensity and depth of turbulent mixing could create the change in the echo at 1625. Barker (1977) (ref 12) showed that strong stability is required at the cloud top to prevent stratus cloud dissipation by dry-air entrainment from above. A decrease in the stability in the region immediately above the inversion base after 1625 could explain the echo change.

Several processes, usually present prior to the formation of fog under stratus clouds, are revealed by the acoustic and FM-CW radar echoes in figure 2. Low, thickening stratus clouds were present during the observations in figure 2. Both sounders have weak, thin S echoes from the cloud-top region as discussed above. The strong acoustic U echoes below 200 m (all heights are above MSL) indicate mixing along a strong negative gradient of potential temperature which is often measured by radiosondes at MYF. Weaker, but steady, acoustic echoes between 200 m and the cloud top at 330 m indicate mixing along a near adiabatic temperature gradient often observed in a free-convective region. Intermittent drizzle, originating within 10 m of the cloud-top echo, was observed by the radar throughout this time period. Drizzle (R echo) appears to signify conditions when the stratus cloud base descent rate is near maximum. No FM-CW radar echoes from humidity mixing regions were observed below the cloud top.

b. Ceilometer film records

A rotating beam ceilometer (AN/GMQ 13C) with a 400 ft (122 m) base leg has been operated intermittently at NOSC since September 1975. The output of the ceilometer has been displayed on an intensity modulated scope which was filmed by a 35-mm shutterless movie camera to provide the same type of record made for the FM-CW radar and acoustic

[12] Barker, E.H., 1977: A maritime boundary-layer model for the prediction of fog. Boundary-Layer Meteor., 11, 267-294.

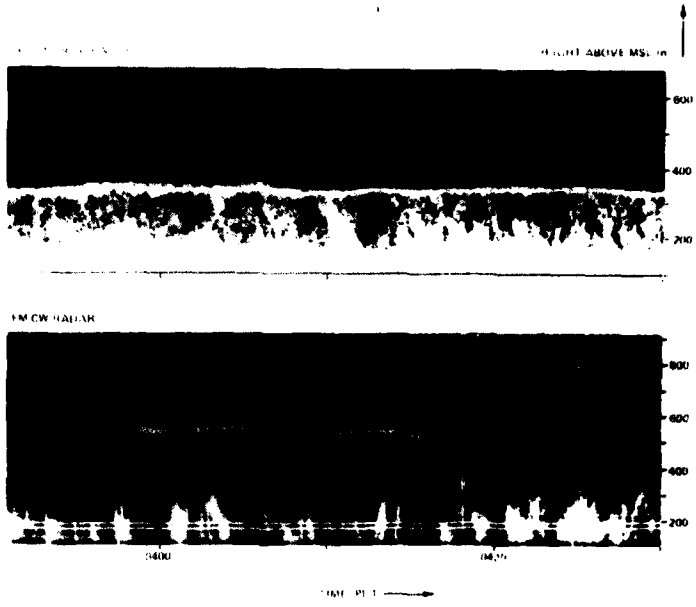

Figure 2. Simultaneous observations on the coast of San Diego when stratus clouds and drizzle were present.

echosounder returns. Figure 3 shows a continuous ceilometer record when a cloud base was descending to create fog. The nonlinearity of the vertical height scale provides considerable detail during low ceiling or near-fog conditions.

The large dynamic range of the filming technique and the automatic gain control of the ceilometer permit considerable detail to be detected in the moist marine layer when clouds are absent or thin. During conditions of minimum signal return, the receiver gain is automatically increased to its maximum; light scattered from small particles can then be detected by the receiver. The change in the gain at the beginning of each vertical sweep depends on the intensity of the return on the preceding sweep. This provides a rapid response relative to the rotation rate of the beam.

Figure 4 shows a ceilometer return during the dissipation of stratus clouds with a base at 90 m. The weak, continuous ceilometer echo region below 90 m after 1315 GMT is created by the presence of haze particles below an inversion capping the clouds when the gain of the ceilometer receiver is at a maximum. The weak, haze-echo layer provides a continuous record of the depth of the moist marine layer bounded near 90 m by an inversion.

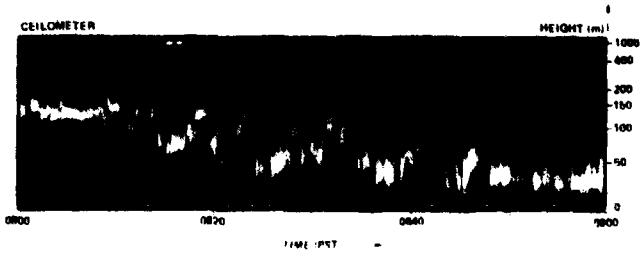

Figure 3. Filmed ceilometer record during the onset of fog.

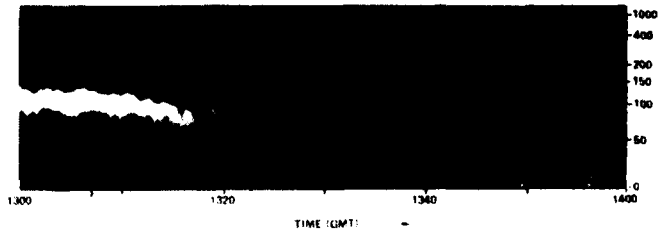

Figure 4. Filmed ceilometer record showing haze layer up to 100 m after stratus clouds dissipated at 1315 GMT.

Haze-layer echoes like these generally weaken as the haze-layer depth increases. This simple ceilometer recording technique has been used to provide continuous cloud-thickness measurements during fog investigations because the acoustic echosounder and the FM-CW radar provide cloud-top heights.

c. Convection over coast

Sensors operated by NOSC on the coast of San Diego on 3 October 1976, observed convective activity in marine air carried over the sensors by northwesterly winds. The sensors observed the vertical growth of a surface-based convective mixing layer from 1200 to 1900 PDT. Thin, scattered clouds formed near 475 m about 6 hr after the commencement of convective activity. Figure 5 shows the film record of the acoustic sounder and FM-CW radar backscatter as a function of elevation and time. Echoes like those below 600 m have been shown by Arnold and Rowland (1976) (ref 13) and Noonkester (1976) (ref 14) to be

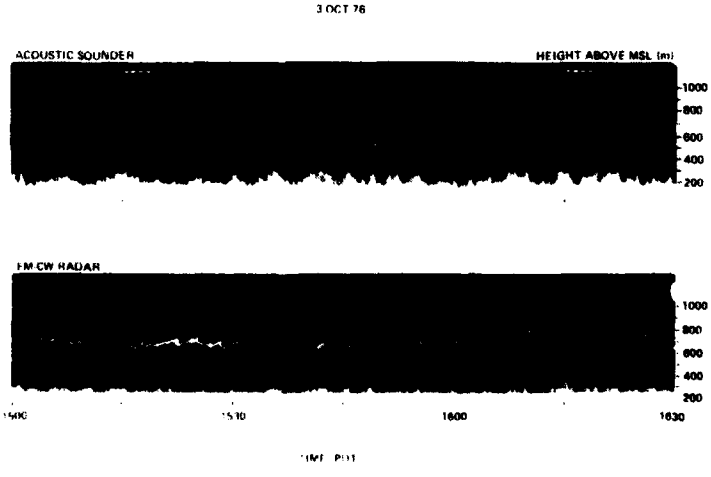

Figure 5. Simultaneous observations on the coast of San Diego during ocean-based convective activity.

[13]Arnold, A. and J.R. Rowland, 1976: Fine scale observations of free convection in the atmospheric boundary layer. Preprints, Third Conf. on Atmos. Turbulence, Diffusion and Air Quality, Raleigh, N.C., Oct 19-22.

[14]Noonkester, V.R., 1976: The evolution of the clear air convective layer revealed by surface-based remote sensors. J. Appl. Meteor., 15, 594-606.

from regions of turbulence caused by surface-based free convection. The echoes near 500 m (C echoes) are from the boundary between plumes of moist air originating from the heated surface and dry air overlying the mixing region. The stronger FM-CW radar echoes near the top are from regions where the rising, buoyant moist air has passed the level of neutral buoyancy and is moist and cold relative to the overlying, more quiescent air (Konrad, 1970) (ref 15) being entrained into the mixed layer. The small dots on the radar record are echoes from insects (I echoes).

The strong acoustic echoes below 300 m (U echoes) are from regions of vigorous mixing in and above the negative vertical gradient of potential temperature created by surface heating. The weak acoustic echoes (C echoes) near 500 m are from the tops of the moist, cold plumes. Echoes are almost absent in the middle of the mixed region because the gradient of potential temperature is near zero.

The near-vertical FM-CW radar echoes extending downward from the top of the mixed region (eg, 1615 PDT in fig. 5) are from regions of moisture mixing between downward moving dry air and upward moving moist air (Noonkester, 1976) (ref 14). This interpretation is supported by the presence of deeper surface-based acoustic U echoes beneath deep radar C echoes and shallow surface-based acoustic U echoes beneath the vertically extending radar echoes (eg, 1615 PDT in fig. 5). Downward moving air columns would tend to suppress the intense surface mixing revealed by the acoustic echoes (Arnold and Rowland, 1976) (ref 13).

The Research Vessel ACANIA, operated by the Naval Postgraduate School, released a radiosonde at 1850 PDT 18 km upwind of the sensors on the coast. The radiosonde showed a surface based superadiabatic layer up to 100 m, and an almost constant θ and mixing ratio w up to 475 m near the convective condensation level. The potential temperature increased above 475 m after an initial change of 0.4 k in a 30 m layer, and w decreased rapidly. The acoustic wind system revealed a wind shear at 475 m (1853 PDT), apparently the top of the mixed layer.

Airborne IR measurements (BARNES PRT-5) of the sea surface temperature by Airborne Research Associates (ARA) over the ocean on several days after 3 October revealed a large region of warm water (about 23°C) upwind of San Diego. The temperature on the R/V ACANIA was 19.5°C at 4 m near 1900 PDT. These data indicate that the convective activity occurred in air several degrees cooler than the water. A positive vertical heat flux of 1.13×10^{-2} Km, s, determined by near surface measurements aboard the R/V ACANIA between 1600 and 2000 PDT, is reasonable for the observed change (acoustic and radar data) in the mixed layer depth from 450 to 580 m during this time period. Both penetrative convection and encroachment, rarely observed, were present during this time period (Davidson and Noonkester, 1980) (ref 16).

MYF radiosondes revealed the descent of a subsidence inversion base from 2 km to 830 m between 0500 and 1700 PDT on 3 October. The acoustic sounder and radar began to receive echoes from the base of the subsidence inversion at 1445 when the base was at 820 m. This echo layer was at 660 m when the MYF radiosonde revealed the inversion base to be at

---

[15] Konrad, T.G., 1970: The dynamics of the convective process in clear air as seen by radar. J. Atmos. Sci., 27, 1138-1147.

[16] Davidson, K.L. and V.R. Noonkester, 1980: Observations of the occurrence of encroachment within the marine atmospheric boundary layer (CEWCOM-76). Preprints Second Conference on Coastal Meteorology, American Meteor. Soc., Los Angeles, CA., 30 Jan to 1 Feb.

830 m, a difference occasionally observed along the coast during the day (sea breeze effect). A MYF radiosonde at 0900 on 4 October showed the base of the subsidence inversion to be at 309 m.

Kelvin-Helmholtz instabilities, KHI (W/echo), were observed at the subsidence inversion base as shown in figure 5. The amplitude of each of these KHI wave trains was 75 to 100 m and the waves passed over the sensor site at a rate of about one every 2 minutes. Relative to the wind direction carrying the KHIs across the sensors, the direction of overriding at the top of the KHIs indicates that the wind speed decreased with elevation for all wave trains. These consistencies indicate that the atmospheric thermal and dynamic structure was nearly constant in the height region spanning the KHIs for over a 2-1/2-hour period.

Investigations (eg. Browning, 1971 (ref 17) and Atlas, et al., 1970 (ref 18) have indicated that the Richardson number Ri must be less than about 0.25 for KHI waves to form. The KHI waves occurred above the height window of the acoustic wind sensing system; thus the wind shear near the waves could not be determined. However, Ri was about 0.25 at 500 m using $\Delta\theta/\Delta z$ from a radiosonde taken at 1850 PDT at the sensor site and using the acoustic wind profile taken at 1817 PDT.

A cloud base was reported by the ARA pilot to be at 475 m near 1730 PDT when clouds began to form in the area. Assuming the mixing layer depth h observed by the sensors represented the cloud top, then the cloud thickness was 30 m at 1730. The ceilometer record indicated that the cloud base was about 430 m at 1830 when h was 530 m and about 375 m at 2100 when h was 600 m. These cloud thicknesses of 30, 100, and 225 m represent an almost linear increase with time. The merger of the convective layer and subsidence inversion occurred at 600 m near 1930. Apparently the convective activity continued to supply moisture to the top of the convective layer in a steady manner regardless of the effects of the subsidence inversion. The clouds dissipated at about 2400 as low-level acoustic and radar echoes essentially dissipated.

d. Convective cell size

Horizontal structure velocity r can be determined at elevation z when echo structures on the scanning radar can be clearly identified on simultaneously measured echoes by the collocated vertically pointing radar and the scan plane is parallel to the horizontal wind vector at elevation z. Using information from one scan only

$$r_1 = \frac{\bar{R}}{1 - (t/s')\,\bar{R}} \qquad (1)$$

and using information from two (near) successive scans in opposing directions

$$r_2 = \left(\frac{t_1 + t_2}{t_1 - t_2}\right)\bar{R} \qquad (2)$$

[17] Browning, K.A., 1971: Structure of the atmosphere in the vicinity of large amplitude Kelvin-Helmholtz billows. Quart. J. Royal Meteor. Society, 97, 283-299.

[18] Atlas, D., J.I. Metcalf, J.H. Richter and E.E. Gossard, 1970: The birth of "CAT" and microscale turbulence. J. Atmos. Sci., 27, 903-913.

The terms are identified in figure 6 for data observed on 8 February 1973 on the San Diego coast. $\bar{R}$ is the average scan velocity at z given by

$$\bar{R} = \left(\frac{\tan\theta_i - \tan\theta_j}{\theta_i - \theta_j}\right)\left(\frac{\Delta\theta}{\Delta t}\right) Z \qquad (3)$$

where $\theta_{i,j}$ is the angle off the vertical of features i,j in equation (1) and is the extreme scan angles (off the vertical) for the full scan in equation (2) and $\Delta\theta/\Delta$ is the angular scan rate. The angle $\theta_{i,j}$ is positive toward the east.

Table 4 gives r, $\bar{R}$ and the expected relative error in r for features identified in figure 6. No measurement of the wind at 350 m above the radars (radars were 33 m above MSL) was available at the sensor site. At 1600 PST a MYF radiosonde measured a wind of about 315° at 15 knots near 380 m. The surface wind at the sensors was 310° at 13 knots. Assuming the wind over the radars was from the NW (315°) at 380 m, the features extended horizontally perpendicular to the wind (features highly similar on fixed and scan records), and the features were moving with the wind at velocity V, then r in table 4 is $V\sec\phi$ where ϕ is 45°. Using 5.5 m/s from table 4 as the best estimate of r during the scans shown in figure 6, the wind velocity V from the NW was 3.9 m/s (7.6 knots) at 383 m. Although a wind velocity of 7.6 knots is only one-half the 1600 PST radiosonde wind of 15 knots near 350 m, the wind speed derived from the radar data is considered representative.

The expected relative error dr/r can be estimated by differentiating equations (1) and (2) and substituting values of $d\bar{R}$, ds', dt, dt_1, and dt_2, the measurement errors (see table 4). The small expected relative error dr/r for the full scan in table 4 suggests the superiority of the full scan method of determining r which uses the maximum s' available. By scanning in the plane of the wind vector and minimizing errors in $\bar{R}$, t_1, and t_2, V can be accurately determined using the full scan method.

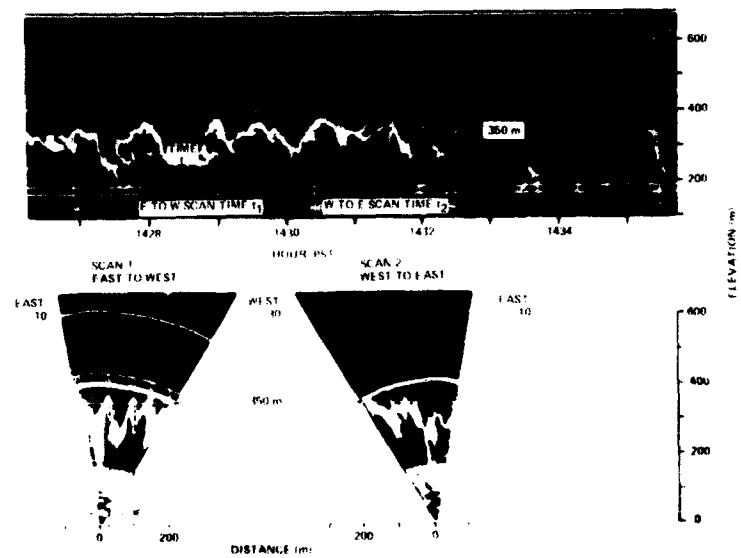

Figure 6. Simultaneous observations on the coast of San Diego during ocean-based convective activity.

Structure Features	m/s $\bar{R}$	m/s r	Expected Relative Error, $\frac{dr}{r}$
B to D	1.3	9.9	± 1.27
E to F	1.5	4.1	± 0.62
F to I	1.4	9.8	± 0.53
Scans 1, 2	1.4	5.5*	± 0.05

*By equation (2). Other r's by equation (1).

Table 4. Horizontal velocity r (positive to the east) of the structures in figure 6 in plane of scan at 350 m elevation according to equations (1) and (2). $\bar{R}$ is average scan velocity at 350 m between structure features. For data shown in figure 6, the approximate measurement errors are: z ± 10 m, $\theta \pm 2°$, $\Delta\theta/\Delta t \pm 0.01°/s$, t ± 3s, and s' ± 10 m.

The echo features in figure 6 were created by surface-based free-convective activity. Assuming the plume tops at 350 m (above radars) represent cool, moist convective air having overshot the neutral buoyancy level by virtue of momentum gained below (Konrad, 1970) (ref 15), the effective depth h of the convective layer is less than 350 m. A depth of 330 m above MSL is assumed to represent h in figure 6.

If features shown in figure 6 at 350 m above the radars are transported from the NW at the deduced rate of 3.9 m/s, then the horizontal dimension of cell B is 234 m. Because the structures observed by the scanning radar and vertically pointing radar are highly similar in figure 6, the features must be almost unmodified in the direction perpendicular to the wind at least out to 200 m from the sensors in the westerly direction. Thus, the horizontal dimension of cell B should be representative of a convective cell carried by the wind and the horizontal dimension of cell B is 0.7 h. Using Fitzjarrald's (1978) (ref 19) relation between scale sizes, h, and stability for ocean data, the convective activity present on 3 February was created by high instabilities.

e. Convective condensation level

Simultaneous observations of a common volume were made by the vertically pointing, fixed FM-CW radar and a lidar during January 1972 (Noonkester, et al., 1974) (ref 6). The lidar was the Stanford Research Institute's Mark VIII ruby lidar (wavelength of 0.694 μm, see table 1) which recorded its backscatter on film like the radar backscatter. A continuous radar echo from the base of the temperature inversion was observed to rise slowly from 200 m at 1220 PST to 300 m by 1420. Low level convective radar echoes began at 1230 and continued until 1350. Figure 7 shows the simultaneous lidar and radar record when strong radar convective echoes were present. Before 1320, the lidar record revealed a relatively homogeneous echo layer up to the base of the temperature inversion (same

[19] Fitzjarrald, D.E., 1978: Horizontal scales of motion in atmospheric free convection observed during the GATE experiment. J. Appl. Meteor., 17, 213-221.

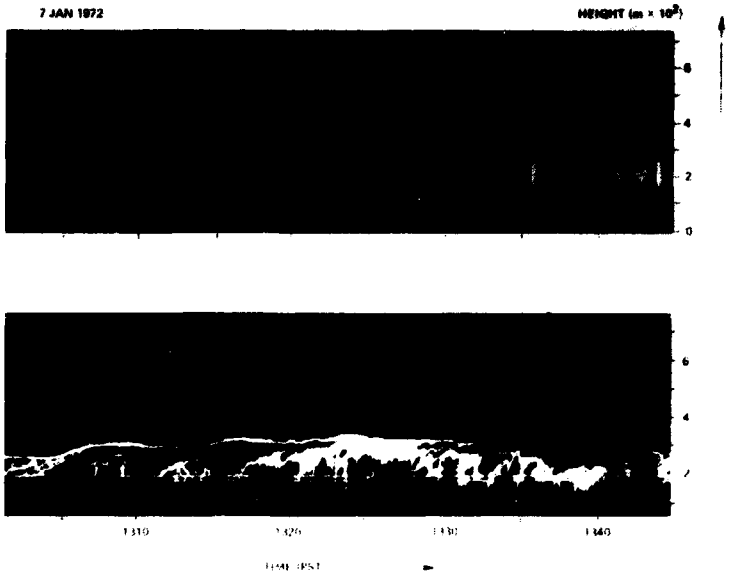

Figure 7. Simultaneous observations by lidar (top) and FM-CW radar (bottom) during ocean-based convective activity. Clouds formed near 1340 PST.

elevation as the continuous radar record) indicating a near uniform distribution of aerosols below the inversion base apparently caused by moderate mixing. At 1320 the lidar record began to reveal stronger echoes in the region of strong convective radar echoes. The intensity of these lidar echoes increased until their intensity indicated the presence of clouds, their bases being below the inversion base at about 180 m. At 1420, the cloud base remained at 180 m and the radar record indicated the cloud top was coincident with the inversion base at 300 m.

Although the lidar and the radar revealed highly similar features (including KHI waves) most of the time during 9 days of simultaneous observations, occasionally the lidar revealed several persistent aerosol layers above the base of a low temperature inversion not observed by the radar.

During September and October 1973, the mobile/scanning FM-CW radar was operated adjacent to an acoustic echosounder 23.2 km north of the high-power radar at Wallops Island, Virginia, to observe surface-based convective activity (Noonkester, 1976) (ref 14). Figure 8 is a graphic presentation of the convective mixed layer depth h during one day when clouds formed. All three sensors revealed the same h although h could not be observed by the acoustic sensor after h passed 800 m and moved above the FM-CW radar window at 1250 m. The high-power radar observed the continued growth of the convective layer until about 1500 EDT.

The convective condensation level was at 1580 m according to the 1118 EDT radiosonde taken at Wallops Island. Scattered clouds were forming at Wallops Island near 1200 m at 1100. The cloud cover near 1200 m was classified as broken at 1400 and was classified as overcast after 1500 at Wallops Island. The increase in h after 1140 could be caused by additional buoyancy added to the rising air by the latent heat of condensation. The addition of moisture at the top of the cloud or mixed layer is evident by the change

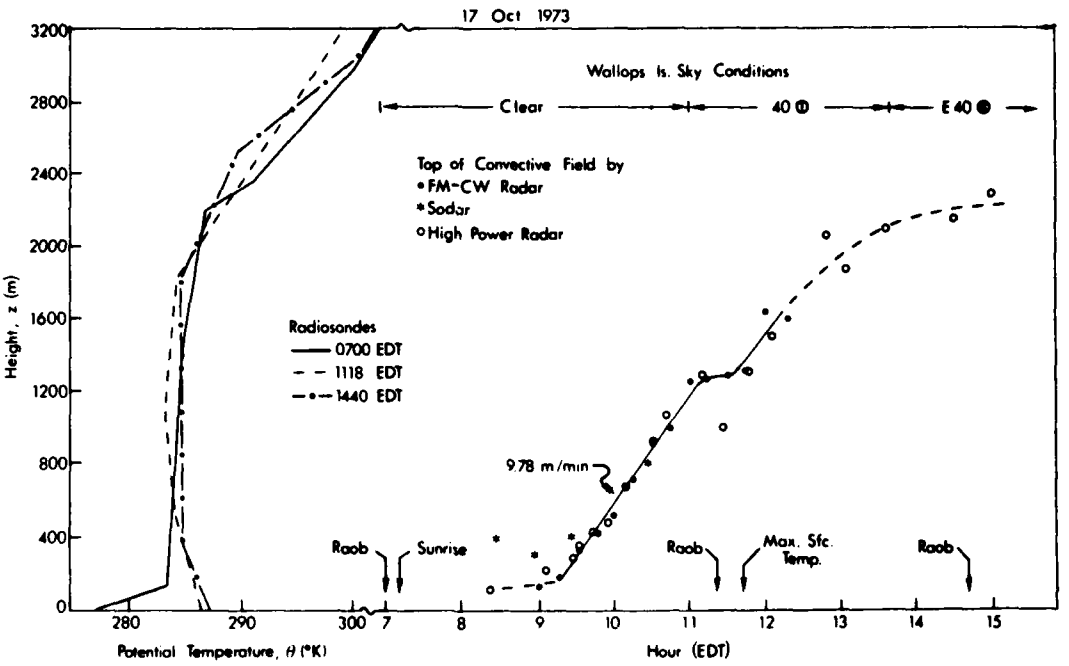

Figure 8. Depth of convective mixed layer during daytime convective activity by three remote sensors near Wallops Island, VA. Meteorological data were taken at Wallops Island, VA.

in relative humidity from 25% (1118 radiosonde) to 81% (1140 radiosonde) at 2200 m. According to these radiosondes, the air above 2700 m apparently warmed by subsidence while the air between 1800 and 2600 m cooled slightly (2.5 K maximum decrease). The cooling is considered to be caused by strong penetrative convection at the top of the cloud layer.

f. Wind shear

Results by Barker (1977) (ref 12) and Oliver, et al. (1978) (ref 20) indicate that moisture transport across the inversion capping a fog or stratus cloud must be small to maintain a cloud/fog deck. Although radiational cooling near the cloud/fog top (Noonkester, 1979b) (ref 21) appears to increase the stability just above the top to reduce the mixing of the moist and dry air, wind shear can occasionally greatly increase the mixing and significantly reduce the moisture in the cloud/fog deck as demonstrated in the example below.

A thin, stratus deck with a base at 90 m preceded fog observed at NOSC near 0000 PDT on 8 October 1976. The stratus dissipated for about 25 min about 1.5 hours before the fog onset when plume-like FM-CW radar echoes appeared for 25 min and extended from 300

[20]Oliver, D.A., W.S. Lewellen and G.G. Williamson, 1978: The interaction between turbulent and radiative transport in the development of fog and low-level stratus. J. Appl. Meteor., 35, 301-316.

[21]Noonkester, V.R., 1979b: Coastal marine fog in Southern California. Monthly Weather Rev., 107, 830-851.

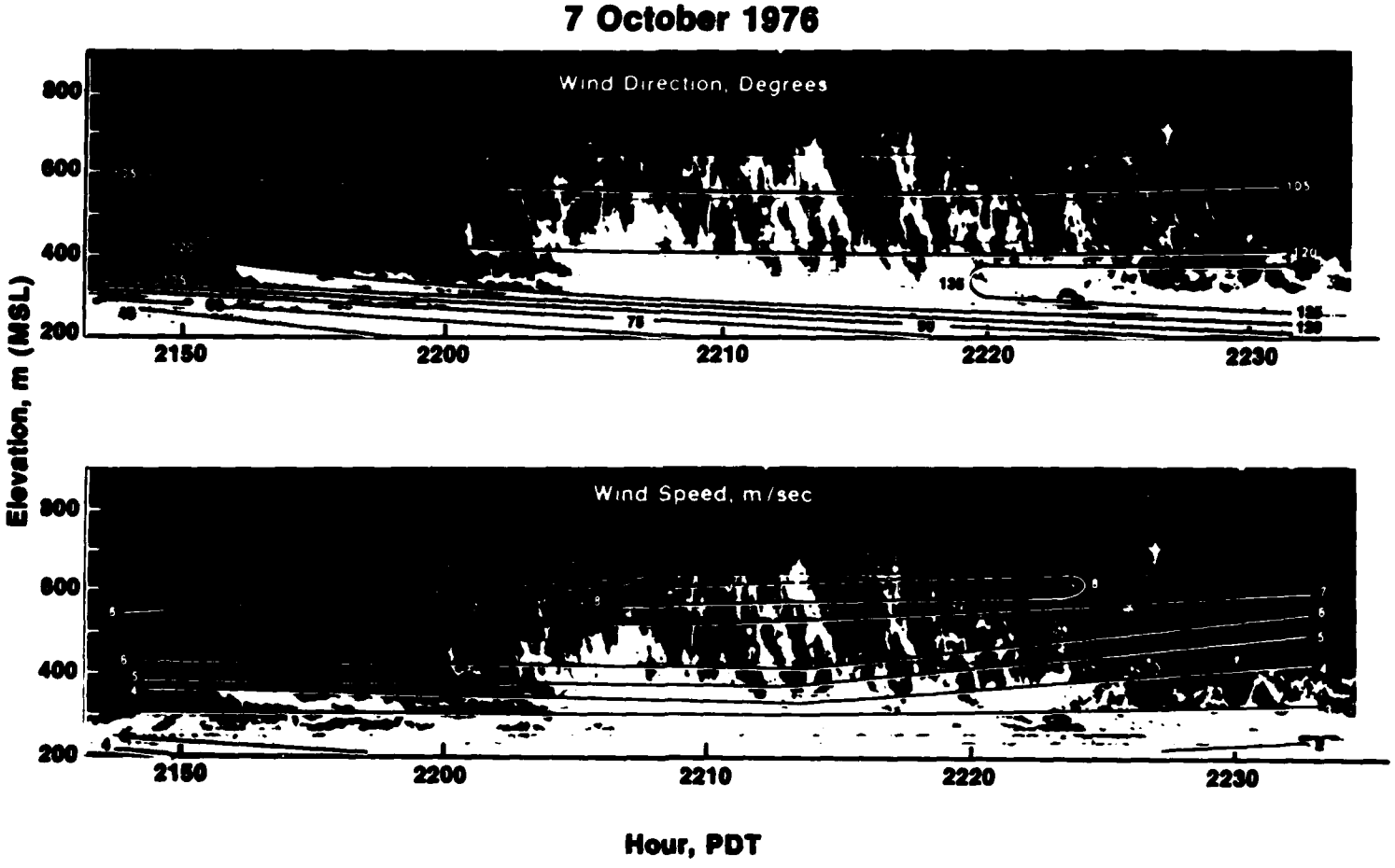

Figure 9. Composite FM-CW radar echoes and wind direction and speed during strong wind shear and stratus dissipation.

to 600 m. The stratus hole and deep echoes occurred almost simultaneously and existed for 25 min. The stratus cloud dissipation and radar echoes were found to be produced by a strong wind shear moving into the stratus deck from above.

A composite presentation of acoustic winds and FM-CW radar echoes during the occurrence of the deep radar echoes and the stratus hole is shown in figure 9. The isopleths were constructed from acoustic wind profiles (7 wind levels) obtained at 2130, 2200, and 2230 PDT. Analysis of the original filmed record of the radar echo reveals that the echo between the 105° and 120° directional isopleths from 2153 to 2200 is a series of KHI waves. Deep, vertically extending echoes suddenly appeared at about 2203 and dissipated by about 2230. These echoes had a structure similar to "plumes" originating from the surface during daytime free convection over land (Noonkester, 1976) (ref 14). The plumes are revealing strong, turbulent mixing of moisture in a deep, dry, stable region up to 600 m.

The relationship between the maximum wind speed axis, the deep radar echoes, the stratus hole and an interpolated potential temperature profile (interpolated between 1700 PDT on 7 October and 0500 PDT on 8 October) is given in figure 10. A wind shear region like the one extrapolated to be near 150 m at 2205 would be expected to create strong mixing of moisture and potential temperature across the inversion base.

OPERATIONAL POTENTIAL

Information on the vertical mixing characteristics near the surface is essential to the understanding of processes controlling important weather elements such as clouds, fog, visibility, aerosol distribution and turbulence. Although the use of the remote sensors described above is not restricted to the coastal region, the extensive measurements by these sensors at the coast have clearly demonstrated their capability to monitor atmospheric mixing processes controlling important low-level weather elements in the coastal region. The use of these sensors in research has been amply demonstrated, but their use in applied problems has not been clearly demonstrated.

An ongoing record of FM-CW radar, acoustic echosounder or lidar echoes could obviously provide considerable information about ongoing mixing processes and, when used in conjunction with normally available meteorological data, could aid in the temporal extrapolation of the outcome of the processes. For example, an estimate of the time of cloud formation can be made by knowing $\Delta h/\Delta t$ if the convective condensation level is known as demonstrated in figure 8. Inversion depth changes aid in forecasting changes in cloud depth, maximum surface temperature, turbulence structure, pollution concentrations, visibility and wind shear. Rapid changes in the depth of subsidence inversions often occur along the California coast and are not adequately monitored by NOAA radiosondes at MYF taken every 12 hours. Multiple layer echoes (wind shear regions) above the base of the subsidence inversion in Southern California usually signal mesoscale changes not revealed by coastal meteorological data. The operational use of these sensors may sometimes be handicapped by the inability to identify echoes related to local, mesoscale and synoptic features. Reliable scale-size identification could permit temporal extrapolation of meteorological processes for appropriate horizontal scales.

Although acoustic echosounders are being used for specific operational problems, the general operational use of surface based remote sensors in coastal or marine air appears to be hampered by cost of sensors (acoustic echosounders are relatively economical), lack of an economical updating recording device capable of revealing details (facsimile often inadequate)

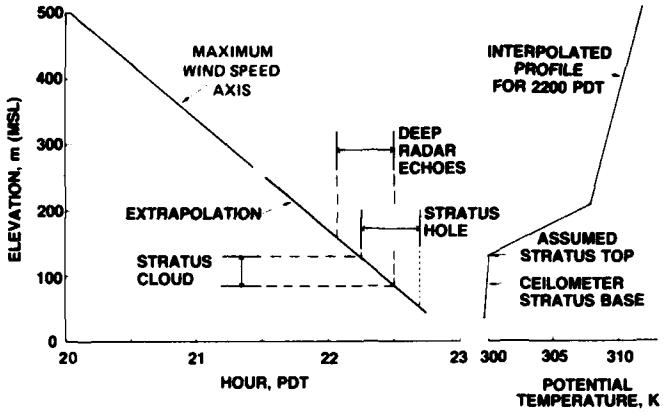

Figure 10. Relationships between wind speed axis, deep FM-CW radar echoes, stratus hole and potential temperature profile on 7 October 1976.

in the echo structure and lack of experience in their operational use. With planned, directed encouragement these sensors could take their place beside other atmospheric sensors for naval operations.

REFERENCES

1. McAllister, L.G., 1968: Acoustic sounding of the lower troposphere. J. Atmos. and Terr. Phys., 30, 1439-1440.

2. Richter, J.H., 1969: High resolution tropospheric radar sounding. Radio Sci., 4, 1261-1268.

3. Beran, D.W., B.C. Willmarth, F.C. Carsey and F.F. Hall, Jr., 1974: An acoustic doppler wind measuring system. J. Acoust. Soc. Am., 55, 334-338.

4. Chadwick, R.B., K.P. Moran, R.G. Strauch, G.E. Morrison and W.C. Campbell, 1976: A new radar for measuring winds. Bull. Am. Meteor. Soc., 57, 1120-1125.

5. Jensen, D.R., and J.H. Richter, 1976: Evaluation of a Xonics Acoustic Echosounder and Wind Sensing System. Naval Electronics Laboratory Center Tech. Report 1997.

6. Noonkester, V.R., D.R. Jensen, J.H. Richter, W. Viezee and R.T.H. Collis, 1974: Concurrent FM-CW radar and lidar observations of the boundary layer. J. Appl. Meteor., 13, 249-256.

7. Richter, J.H., D.R. Jensen, V.R. Noonkester, T.G. Konrad, A. Arnold and J.R. Rowland, 1974: Clear air convection: A close look at its evolution and structure. Geophys. Res. Lett., 4, 173-176.

8. Noonkester, V.R., 1979a: A technique for coding boundary layer echoes from surface-based remote sensors. Bull. Am. Meteor. Soc., 60, 20-27.

9. Richter, J.H., D.R. Jensen and M.L. Phares, 1972: Scanning FM-CW radar sounder. The Review of Scientific Instruments, 43, 1623-1625.

10. Wesely, M.L., 1976: The combined effect of temperature and humidity fluctuations on refractive index. J. Appl. Meteor., 15, 43-49.

11. Gossard, E.E., D.R. Jensen and J.H. Richter, 1971: An analytical study of tropospheric structure as seen by high-resolution radar. J. Atmos. Sci., 28, 794-807.

12. Barker, E.H., 1977: A maritime boundary-layer model for the prediction of fog. Boundary-Layer Meteor., 11, 267-294.

13. Arnold, A., and J.R. Rowland, 1976: Fine scale observations of free convection in the atmospheric boundary layer. Preprints, Third Conf. on Atmos. Turbulence, Diffusion and Air Quality, Raleigh, N.C., Oct 19-22.

14. Noonkester, V.R., 1976: The evolution of the clear air convective layer revealed by surface-based remote sensors. J. Appl. Meteor., 15, 594-606.

15. Konrad, T.G., 1970: The dynamics of the convective process in clear air as seen by radar. J. Atmos. Sci., 27, 1138-1147.

16. Davidson, K.L., and V.R. Noonkester, 1980: Observations of the occurrence of encroachment within the marine atmospheric boundary layer (CEWCOM-76). Preprints Second Conference on Coastal Meteorology, American Meteor. Soc., Los Angeles, CA, 30 Jan to 1 Feb.

17. Browning, K.A., 1971: Structure of the atmosphere in the vicinity of large amplitude Kelvin-Helmholtz billows. Quart. J. Royal Meteor. Society, 97, 283-299.

18. Atlas, D., J.I. Metcalf, J.H. Richter and E.E. Gossard, 1970: The birth of "CAT" and *microscale turbulence*. J. Atmos. Sci., 27, 903-913.

19. Fitzjarrald, D.E., 1978: Horizontal scales of motion in atmospheric free convection observed during the GATE experiment. J. Appl. Meteor., 17, 213-221.

20. Oliver, D.A., W.S. Lewellen and G.G. Williamson, 1978: The interaction between turbulent and radiative transport in the development of fog and low-level stratus. J. Appl. Meteor., 35, 301-316.

21. Noonkester, V.R., 1979b: Coastal marine fog in Southern California. Monthly Weather Rev., 107, 830-851.

DOCUMENTATION, CHRONOLOGICAL

Gossard, E.E., J.H. Richter and D.R. Jensen, Dynamic Stability of Atmospheric Waves, NELC TR 1813, Jan 1972.

Richter, J.H. and D.R. Jensen, Remote Sensing of the Lower Atmosphere by Means of FM-CW Radar, NELC TR 1845, Sep 1972.

Noonkester, V.R., D.R. Jensen and J.H. Richter, "Simultaneous FM-CW Radar and Lidar Observations," Preprints: 15th Radar Meteorology Conference, p 335-340, 10-12 Oct 1972.

Noonkester, V.R., D.R. Jensen and J.H. Richter, Simultaneous FM-CW Radar and Lidar Probing of the Atmosphere, NELC TR 1849, 1 Nov 1972.

Richter, J.H., D.R. Jensen and M.L. Phares, "Scanning FM-CW Radar Sounder," Rev. Sci. Inst., v 43, p 1623-1625, Nov 1972.

Richter, J.H., D.R. Jensen and V.R. Noonkester, "Scanning FM-CW Radar Sounder," Preprints: 15th Radar Meteorology Conference, 331-334, 1972.

Gossard, E.E. and J.H. Richter, "FM-CW Radar Studies of Production of Turbulent Instability within Thermally Stratified Stable Layers of Internal Waves," AGARD Conference Proceedings no. 115 on Effects of Atmospheric Acoustic Gravity Waves on Electromagnetic Propagation, p 20-1 to 20-14, 1972.

Richter, J.H., E.E. Gossard and D.R. Jensen, "Fine Structure of the Lower Atmosphere as Seen by High Resolution Radar," Proc. Workshop on Mathematics of Profile Inversion, NASA TM X-62, 150; p 2-23 to 2-30, 1972.

Richter, J.H. and D.R. Jensen, "Radar Cross-Section Measurements of Insects," Proc IEEE, v 61, p 1, Jan 1973.

Noonkester, V.R., D.R. Jensen and J.H. Richter, Meteorological Processes and FM-CW Radar Soundings in the Boundary Layer, NELC TR 1862, 5 Feb 1973.

Noonkester, V.R., Distortion and Reconstruction of Low-Level Atmospheric Echoes Obtained by a Scanning Radar, NELC TN 2330, 26 Mar 1973.

Richter, J.H., D.R. Jensen, R.A. Pappert and V.R. Noonkester, "New Developments in FM-CW Radar Sounding," Bound. Layer Met., v 4, p 179-199, Apr 1973.

Gossard, E.E., J.H. Richter and D.R. Jensen, "Effect of Wind Shear on Atmospheric Wave Instabilities Revealed by FM-CW Radar Observations," Bound. Layer Met., v 4, p 113-131, Apr 1973.

Munk, W.H., J.D. Woods, W.P. Birkemeier, C.G. Little, R.H. Stewart and J.H. Richter, "Remote Sensing of the Ocean," Bound. Layer Met., v 5, Apr 1973.

Richter, J.H., D.R. Jensen, V.R. Noonkester, J.B. Kreasky, M.W. Stimmann and W.W. Wolf, "Remote Sensing: Atmospheric Structure and Insects," Science, v 180, p 1176-1178, Jun 1973.

Noonkester, V.R., "Breaking Wave Characteristics Determined from FM-CW Radar Observations," Bull. AMS, v 54, p 937-941, Sep 1973.

Jensen, D.R., V.R. Noonkester and J.H. Richter, Atmospheric Structure Observed by FM-CW Radar at the Salton Sea in the California Desert, NELC TR 1915, 11 Mar 1974.

Noonkester, V.R., D.R. Jensen, J.H. Richter, W. Viezee and R.T.H. Collis, "Concurrent FM-CW Radar and Lidar Observations of the Boundary Layer," Jour. Appl. Meteor., v 13, p 249-256, Mar 1974.

Noonkester, V.R., Convective Activity Observed by FM-CW Radar, NELC TR 1919, 10 May 1974.

Austin, L.B., AGCS and V.R. Noonkester, Statistics on Surface-based Superadiabatic Layers over the Ocean near Southern California, NELC TN 2678, 26 Jul 1974.

Jensen, D.R. and J.H. Richter, FM-CW Radar Observation of Atmospheric Structure in the South San Francisco Bay Area, NELC TN 2763, 12 Aug 1974.

Richter, J.H., D.R. Jensen, V.R. Noonkester, T.G. Konrad, A. Arnold and J.R. Rowland, "Clear Air Convection: A Close Look at Its Evolution and Structure," Geophys. Res. Lett., v 1, p 173-176, Aug 1974.

Noonkester, V.R., J.H. Richter and D.R. Jensen, Unique Echoes Observed by FM-CW Radar at a Jet Airport, NELC TN 2787, 13 Sep 1974.

Arnold, A., J.R. Rowland, T.G. Konrad, J.H. Richter, D.R. Jensen and V.R. Noonkester, "Simultaneous Observations of Clear Air Convection by a Pulse Radar, an FM-CW Radar, an Acoustic Sounder, and an Instrumented Aircraft," Preprints: 16th Radar Meteorology Conference, p 290-295, Apr 1975.

Richter, J.H. and D.R. Jensen, "Simultaneous Acoustic Sounder and FM-CW Radar Observations," Preprints: 16th Radar Meteorology Conference, p 282-290, Apr 1975.

Richter, J.H., "High Resolution Radar for Remote Atmospheric Sensing," Proc. IEEE Intl. Radar Conf., p 235-240, Apr 1975.

Noonkester, V.R. and D.R. Jensen, "The Growth and Decay of the Convective Field Revealed by Surface-based Remote Sensors," Preprints: 16th Radar Meteorology Conf., Houston, TX, p 204-311, 22-24 Apr 1975.

Noonkester, V.R., The Evolution of the Clear Air Convective Layer Revealed by Surface-based Remote Sensors, NELC TR 1971, 5 Dec 1975.

Jensen, D.R., Properties of the Marine Boundary Layer Observed by FM-CW Radars at Vandenberg Air Force Base and San Diego, NELC TN 3143, 25 Mar 1976.

Noonkester, V.R., "The Evolution of the Clear Air Convective Layer Revealed by Surface-based Remote Sensing," J. Appl. Meteor., v 10, p 594-607, Jun 1976.

Noonkester, V.R. and L.E. Logue, Fog Related to Stratus Clouds in Southern California, NELC TR 1989, Jul 1976.

Noonkester, V.R., J.H. Richter and D.R. Jensen, "Meteorological Interpretation of FM-CW Radar and Acoustic Sounder Echoes in a Coastal Environment," Preprints: Conference on Coastal Meteorology, Virginia Beach, VA, p 20-27, 21-23, Sep 1976.

Richter, J.H., D.R. Jensen and V.R. Noonkester, "A Coastal Multi-Sensor Measurement Facility at San Diego," Preprints: Conference on Coastal Meteorology, Virginia Beach, VA, p 35-42, 21-23 Sep 1976.

Noonkester, V.R., J.H. Richter and D.R. Jensen, "Marine Fog Investigations in San Diego," Preprints: 17th Conference on Radar Meteorology, Seattle, WA, p 282-289, 26-29 Oct 1976.

Noonkester, V.R. and L.E. Logue, Fog Related to Santa Ana Conditions in Southern California, NELC TR 2000, Nov 1976.

Noonkester, V.R., EO Meteorology and Acoustical Measurement of the Temperature Structure Function C_T, NELC TN 3296, Jan 1977.

Noonkester, V.R., Meteorological Visibility and EO Systems, NOSC TN 167, May 1977.

Delaney, B.T., V.R. Noonkester and J.O. Ledbetter, "Remote Sensing of Aircraft Wake Vortex Movement in the Airport Environment," 70th Annual Meeting of the Air Pollution Control Association, Paper no. 77-41.4, Toronto, Ontario, Canada, 20-24 Jun 1977.

Noonkester, V.R., Marine Fog Investigations at San Diego during CEWCOM-76, NOSC TR 172, Oct 1977.

Noonkester, V.R., "Multi-platform Marine Fog Study," Bull. AMS, v 50, p 1226-1227, Nov 1977 (by-line not given).

Noonkester, V.R., "Multi-Sensor Measurements of Ocean-Based Convective Activity," Preprints: 18th Conference on Radar Meteorology, Atlanta, GA, p 55-64, 28-31 Mar 1978.

Noonkester, V.R., "Acoustic Echosounder, Acoustic Bistatic Wind and FM-CW Radar Measurements during West Coast Foehn Winds," Preprint: 4th Symposium on Meteorological Observations and Instrumentation, Denver, CO, p 447-454, 10-14 Apr 1978.

Noonkester, V.R., "Cloud and Fog Studies Using Remote Sensors in San Diego," Preprint: Conference on Cloud Physics and Atmospheric Electricity, p 215-224, Issaquah, WA, 31 Jul-4 Aug 1978.

Noonkester, V.R., "A Technique for Coding Boundary Layer Echoes from Surface-based Remote Sensors," Bull. AMS, v 60, p 20-27, Jan 1979.

Noonkester, V.R., "Coastal Marine Fog Studies in Southern California," Monthly Weather Rev., v 107, p 830-851, Jul 1979.

Davidson, K.L. and V.R. Noonkester, "Observations of the Occurrence of Encroachment within the Marine Boundary Layer (CEWCOM-76)," Preprints: 2nd Conference on Coastal Meteorology, p 284-287, Los Angeles, CA, Jan 1980.

Noonkester, V.R. and J.H. Richter, "FM-CW Radar Sensing of the Lower Atmosphere," Rad. Sci., v 15, p 337-353, Mar-Apr 1980.